A MODULAR MICROFABRICATION APPROACH WITH MULTI-LAYER MICROPILLAR 3D INTERCONNECTS, UTILIZING DLP 3D PRINTING TOWARDS 3D MICROELECTRODE ARRAYS AND COMPLEX MICROSYSTEMS

Charles M. Didier[1], Avra Kundu[1], and Swaminathan Rajaraman[1]
[1] University of Central Florida, USA

ABSTRACT

In recent years, 3D printing has enabled multitudes of innovation and advances across scientific disciplines. This statement additionally holds true for the field of *in vitro* biological systems. Resin-based 3D printing (such as Digital Light Processing or DLP 3D Printing) have enabled resolutions of features in the low micrometer-scale, a key for 3D Microelectrode Array (MEA) technology. However, most 3D printed approaches are geared towards monolithic approaches. Here, we demonstrate a modular approach to the microfabrication of 3D MEAs, enabled by *unique micropillar interconnects*, which were fabricated through DLP 3D printing. Conductive silver epoxy and thin film deposition is utilized for a combination packaging approach. The device is subsequently characterized for its print resolution, microelectrode materials and 3D MEA impedance performance.

KEYWORDS

Digital Light Processing (DLP) 3D Printing, 3D MEA, Modular, *In Vitro*, Packaging, Computer Aided Design (CAD).

INTRODUCTION

In vitro systems for biological models are largely *either* customizable or cost-effective. Additionally, the requirement for utilization of 3D microelectrodes-based sensing has been established for more complex microphysiological systems (MPS) research, in areas such as neural and cardiac tissue models **[1]**. With the advent of 3D-printing however, novel strategies have resulted in the ability to balance these requirements, and produce innovative sensor designs to meet biological demand and challenges. The emerging MPS field, is reliant in part by advances in the underlying sensing/stimulation platform technologies. Sensors such as 3D MEAs, can be used to obtain signals from electrogenic cell populations **[2,3]**. Key variable-aspect-ratio interconnect microtowers are integral not only to 3D MEAs (described herein) but additionally for *in vitro* drug dispersal mechanisms **[4]**, magnetically-enhanced micro-robotics **[5]**, and microstructures towards MEMS antennae **[6]**, all of which can be enabled by novel 3D-printing techniques **[7]**. Resin or metal-based 3D-printing methods provide a material canvas onto which other functionalization methods may be incorporated, expanding such non-traditional technologies towards more complex microsystems fabrication.

Previously, our work has demonstrated rapid and cost-effective realization of 3D printed 3D MEAs, along with the methods to ensure their biocompatibility **[8,9]**. Herein, Digital Light Processing (DLP) 3D-printing based microfabrication of defined micropillar 3D through-vias is showcased in modular substrates, as a custom approach for development of an independent and modular 3D MEA. The final fabricated MEA is subsequently characterized for its constituent fabricated components (i.e., resolved positive and negative relief features), as well as for its electrical performance through a full spectrum impedance spectroscopy and microelectrode material definition.

MATERIALS AND METHODS

Solidworks CAD (Dassault Systemes, France) was utilized to design the 3D printed components (**Figures 1-2**), which were fabricated with Pro3dure GR-1 clear resin (Pro3dure, Germany), on

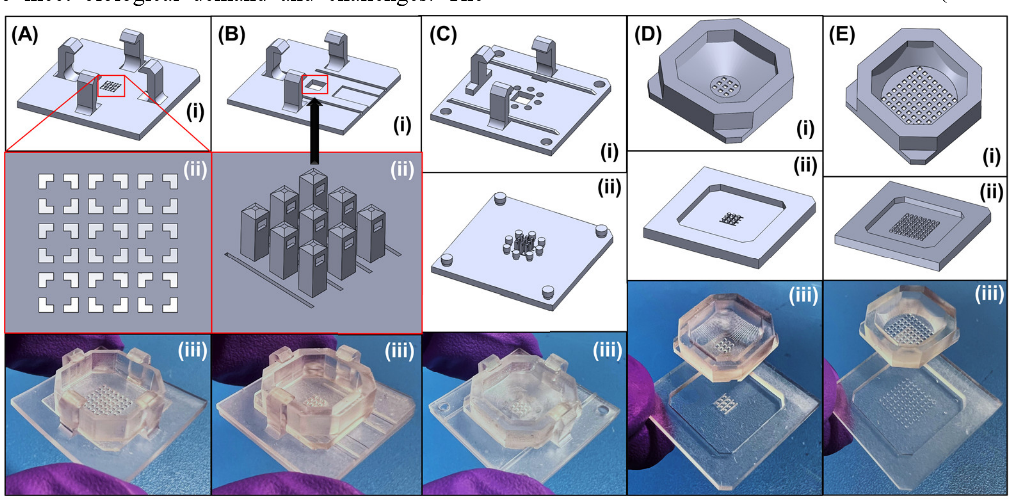

Figure 1 (left): *Iterative sample prototyping* ***[8]*** *for the Modular MEA platform. (A) Original "clipping" substrate (i) containing "plus-shaped" vias (ii) for transitioning "plus-shaped" vias from the attached culture well (iii). (B) Next iteration, which added a sliding mechanism for slotting the culture well (i), along with introducing the micropillar 3D interconnects and laser-isolation relief structures in a third layer (ii). The final 3D electrodes (iii) however did not make robust connection with the micropillars. (C) In the next iteration, "raised slide rails" and "snap-button clips" (i) were introduced to better attach the micropillar substrate (ii) once the culture well was in place (iii). (D) In this iteration,* ***which is detailed fully in this work****, the design was reduced to two components, consisting of the sloped culture well (i) for more directed cell plating, and the recessed micropillar substrate (ii). Once printed (iii), this would allow for a tight-fitting, interchangeable culture well. (E) To demonstrate scalability of the approach in (D), a 64- channel, 8x8 design was additionally prototyped.*

978-1-940470-04-7/HH2022/$25©2022TRF
DOI 10.31438/trf.hh2022.100

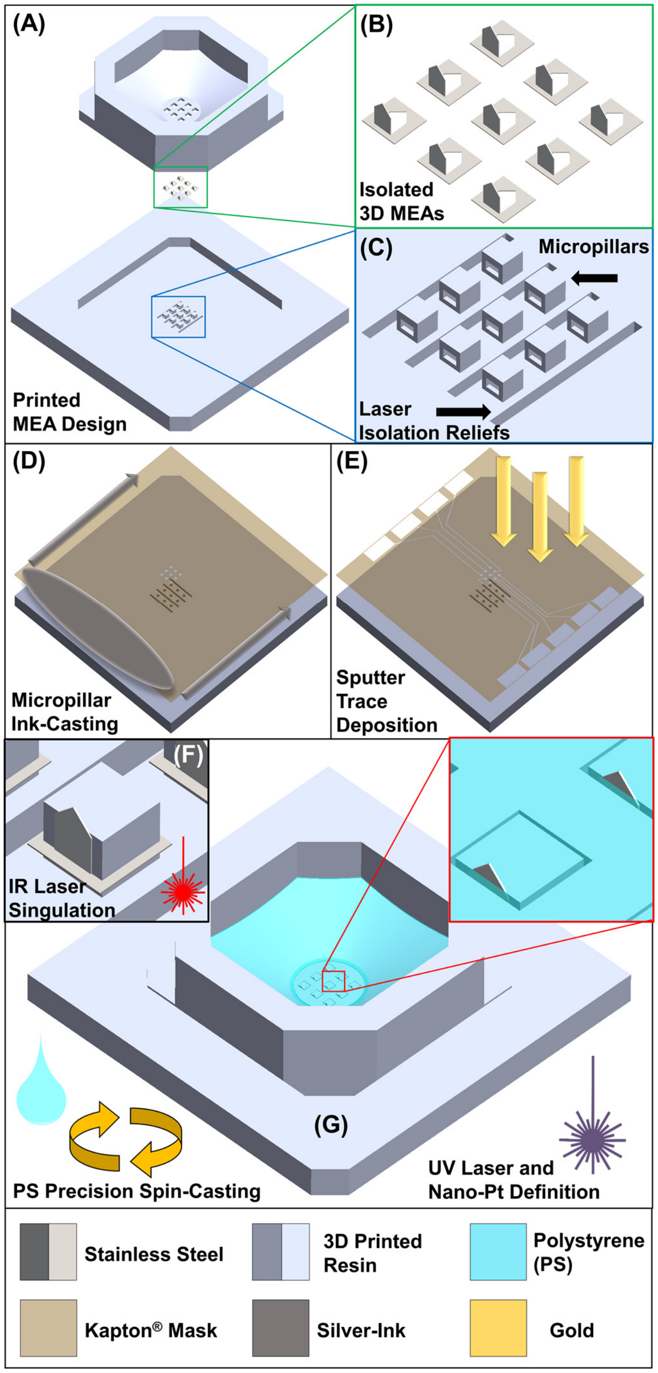

Figure 2: *Modular 3D MEA fabrication schematic (3x3 array). (A) Central components of the MEA platform, including the sloped culture well, the micropillar substrate and the array of SS electrodes between them. (B) Enlarged, isolated SS electrodes. (C) Enlarged schematic of the micropillar substrate, showing the opening of the "inverted-L" vias which would provide silver-ink contact with the micromachined SS electrodes, as well as the laser-isolation reliefs. (D) Illustration of the ink casting process, through the Kapton® mask. (E) Representation of the sputter deposition process through a secondary Kapton® mask after removal of the ink-casting mask. (F) Enlarged schematic which shows the flush connection of the 3D microelectrodes with the micropillar interconnects. (G) Schematic of the assembled and insulated 3D MEA, additionally showing an enlarged schematic of the assembled modular 3D MEA, with the SS electrodes emerging from the partitions in the culture well.*

Asiga MAX X, UV27 DLP 3D-printer at a wavelength of λ=385nm (ASIGA, Australia). Substrate dimensions were defined as: 24mm (length) by 24mm (width) by 2mm (thickness), with a central cut-out of: 16mm (length) by 16mm (width) by 1.3mm (depth). A 3x3 array of micropillars, with dimensions of 400µm (length) by 400µm (width) and 400µm (height), were centrally incorporated with 325µm (length) by 325µm (width) by 1000µm (height), "inverted-L" vias through the micropillars/substrate. Laser-isolation vias (dimensions: 240µm (width) by 3mm (length)) were additionally designed between the rows of micropillars.

The 16mm (length) by 16mm (width) by 8mm (height) interlocking culture well (2mm thick sidewall) was designed in CAD and printed separately, utilizing the same DLP printing. A 3x3 matrix, of 500µm (length) by 500µm (width) openings were incorporated in the culture well, to accommodate the slotting of micropillars and microelectrodes. All prints were subsequently washed in 70% Isopropanol (IPA), and dried before UV-curing to ensure both biocompatibility and proper final print curing **[9,10]**. A modified "Hypo-Rig" assembly (patent-pending **[8,11]**) was similarly designed, printed, and finished, before being fitted with 30G dispensing needles (BSTEAN, USA) for 2D-3D microelectrode transition (**Figure 3A, B**).

3D microelectrodes were IR-laser micromachined (QuickLaze, USA) from 316L stainless-steel (SS) (12.5µm thick) in a 3x3 configuration, with each 2D structure having dimensions of 300µm (width) and 350µm (height) with a 1mm pitch. Horizontal scribe lines between each row of the array were laser defined to allow for full isolation using the integrated laser scribe-vias post-assembly. The SS arrays were subsequently acid-pickled to remove laser debris and other irregularities **[12]**. The array was then aligned and affixed to the back of the culture well, before being transitioned from 2D to 3D utilizing the Hypo-Rig. The culture well / 3D MEA assembly was then aligned and attached to the micropillars on to the base substrate. The micropillars were precisely filled with silver-ink utilizing a UV laser-defined Kapton® (DuPont, USA) shadow mask and then cured at 60°C. To form the contact pads and traces, 30nm of gold was sputtered through a separate Kapton® mask to connect with the bottom sides of the ink-filled vias. A 10µm thick polystyrene insulation was spin-coated inside the assembled culture well and cured at 60°C, before utilizing controlled burst, selective UV-laser micromachining to expose an opening. Nano-porous platinum (N-P Pt.) electroplating was then performed on the laser-exposed electrodes, to increase the functional surface area **[13]**. Full spectrum (100Hz-40MHz) impedance and phase were obtained utilizing the Bode 100 (Omicron Labs, USA), with phosphate buffered saline as the electrolyte and utilizing a Pt anode. Imaging was performed with scanning electron microscopy (SEM; Zeiss, Germany), laser confocal microscopy (Keyence, Japan), and optical modalities (iPhone XS; Apple, USA).

RESULTS AND DISCUSSIONS

Figure 1 illustrates how iterative sample prototyping **[8]** is utilized to quickly change designs during the process development phase. Once an established design is ready to move forward to evaluations, a full microfabrication strategy is designed and deployed (**Figure 2**). "Hypo-Rig" ensures a uniform 2D-3D transition of the SS microelectrodes and the ability to do throughout the array simultaneously (**Figure 3A, B**). The final fabricated device and the laser micromachined array are shown in **Figure 3C, D**.

In-situ impedance characterization was performed during the characterization of the final device, to delineate between "open circuit", SS and N-P Pt. microelectrodes **[14]**. Once electroplating of the microelectrode sites was completed, Energy Dispersive X-ray Spectroscopy (EDS) was performed to confirm the presence and

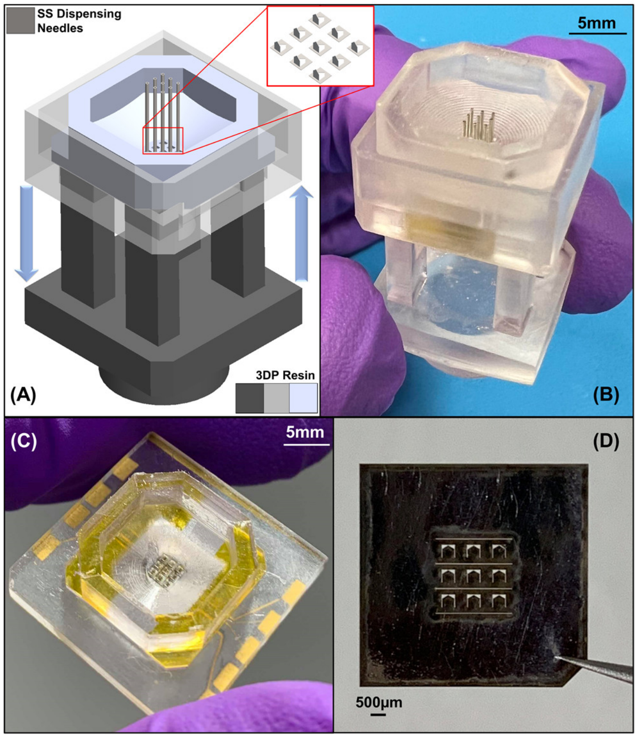

Figure 3: *Schematic and optical images for the custom Hypo-Rig and final Modular 3D MEA. (A) Schematic of the custom Hypo-Rig construct **[8,11]**. The enlarged inset details the 2D-3D transition of the microelectrodes. Integrated slots allow for rapid release of the transitioned array. The included release press is designed to fit evenly to provide uniform force distribution when releasing the culture well and transitioned microelectrodes. (B) Optical image showing the fabricated Rig from (A). (C) Optical image of the full fabricated Modular 3D MEA, schematically detailed in **Figure 2**. (D) Optical image of a closer view of the precision laser micromachined bulk SS before attachment and 2D-3D transition on the Rig.*

uniformity of the N-P Pt., and impedance scans were obtained again. The 1kHz impedance and phase values of **500 kΩ and -9º** respectively, indicate a suitable microelectrode for biological applications when compared to the initial *in situ* values of 25.0 MΩ, with a phase of -50º (not shown) obtained on SS 3D electrodes by precision laser de-insulation of the microelectrode recording sites. This high impedance was indicative of high oxidation of SS, prior to acid pickling **[12]**. The N-P Pt electroplating is used to enhance 3D microelectrode material electrical performance to an acceptable level **[13, 14]**, as shown in **Figure 4A, B**. A Randles equivalent circuit provided relevant extracted circuit parameters for the N-P Pt. microelectrode and are as follows: solution resistance (R_S) of 180Ω, charge transfer resistance (R_{CT}) of 430Ω, double layer capacitance (C_{DL}) of 4.5pF, and the Warburg coefficient (σ) of 10 x 10^4 $\Omega(s^{-1/2})$, which fall well within reasonable expected values (**Figure 4C**) **[15]**.

From the EDS spectrum obtained for the nano-porous platinum microelectrodes (**Figure 4D**), the presence of Au is expected (due to the sputtering for sample preparation for SEM), and the expected peaks for Pt can be clearly observed, confirming the electroplating of the nano-porous material. The inset in **Figure 4D** shows an SEM image of the N-P Pt. plated microelectrode, illustrating the success of the controlled burst laser ablation of the electrode tip to remove the insulation and the growth of N-P Pt. electrode material. Such a material increases the functional surface area of the microelectrode, without adding to the drawn electrode area, thereby reducing the impedance as demonstrated here.

Combination image analysis was utilized to assess the design to device translation of positive and specifically sensitive negative relief features. While SEM results detailed resolution of positive micropillars, laser confocal imaging allows for precise analysis of negative vias. Optically, the prints match the CAD designs closely (**Figure 5A**). However, under the SEM, it can be observed how curing of the resin during printing may "over-cure" the resin producing rounded corners. If print parameters are not carefully controlled, these errors may propagate throughout the printing process and cause closure of sensitive negative features **[9]**. For SEM imaging (**Figure 5B, C**), top most layers of the micropillars from printing to both illustrate the defined DLP layers, as well as to allow for better analysis of potential internal defects. As may be observed, some via closure is observed, but no major error propagation can be noticed. With respect to the laser confocal analysis (**Figure 5D, E**), the top layers of the micropillar interconnects were removed so that the system could properly interrogate the sensitive negative features of interest. Quantitatively, the values extracted from the laser confocal imaging were all within acceptable margins of error. The foundational ink via width / lengths (forming the base to the micropillars) were designed to be **325µm** and resolved across various prints **at 320.18 +/- 7.13µm**. Laser isolation via width were designed to be **240µm** and resolved to be **231.35 +/- 7.13µm**. The depth of the ink-casting vias was designed at **700µm** which was the depth of the center of the substrate and was measured as **696.15µm +/- 68.66µm**. While the error here is larger, it can be attributed to inconsistencies in the stage under the substrates which would lead to variations in measured depth. Finally, the surface roughness was measured at **1.37 +/- 0.22µm**, which ensures well connected culture well.

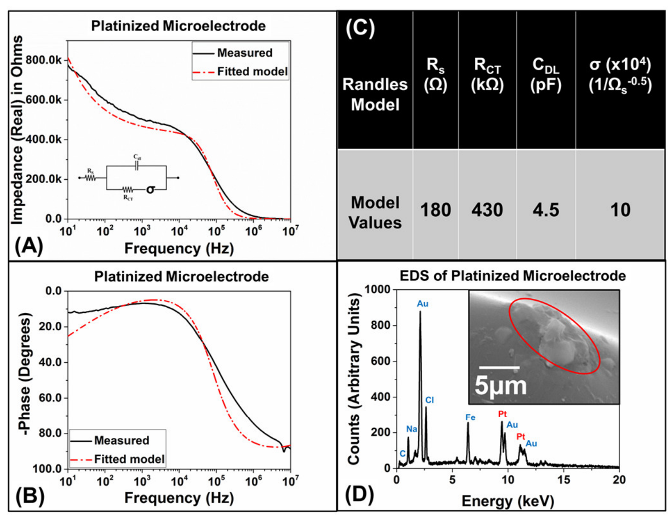

Randles Model	R_s (Ω)	R_{CT} (kΩ)	C_{DL} (pF)	σ (x10^4) ($1/\Omega_s^{-0.5}$)
Model Values	180	430	4.5	10

Figure 4: *Microelectrode characterization for the Modular 3D MEA platform. (A-C) Full spectrum (100Hz-40MHz) impedance and phase characterization, with a Randles' equivalent circuit fitting for extracting relevant parameters. Impedance (A) and phase (B) of the nano-porous platinum plated 3D microelectrode recording sites. The 1kHz impedance and phase values of **500 kΩ** and **-9º** are well within literature defied values. A custom Randles' circuit is shown as an inset (A), and the resulting fitting is graphed in red. Relevant parameters have been extracted from this model and are detailed in (C). (D) EDS spectrum of the nano-porous platinum microelectrodes.*

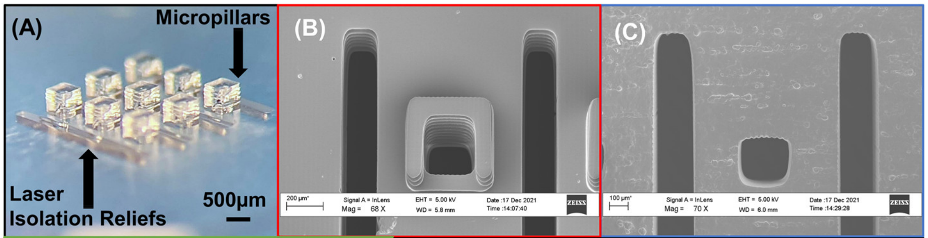

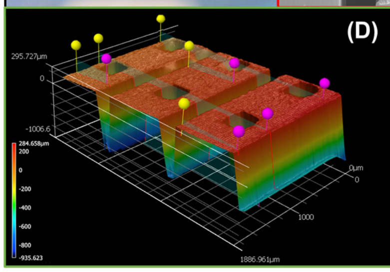

(E)	Ink Via *Width* / *Length*	Laser Isolation Via *Width*	Substrate Via *Depth* (Under Micropillar)	Surface Roughness
CAD Design Dimensions	325µm	240µm	700µm	N/A
Laser Confocal Dimensions	320.18um +/- 7.13µm	231.35 +/- 7.13µm	*696.15um +/- 68.66µm	1.37µm +/- 0.22µm

Figure 5: *SEM and laser confocal imaging for design to device translation analysis of positive and sensitive negative via features. (A) Enhanced optical image of the micropillar substrate indicating the positive structures as well as the laser isolation reliefs. (B&C) SEM images of the top (B) and bottom (C) of the micropillar substrate. The top of the micropillars in (B) were omitted from this chosen print to illustrate the defined DLP layers. (D) Laser confocal scanning image of a representative section of the micropillar substrate. (E) Quantitative values extracted from the laser confocal imaging from (D), where all values are within acceptable error margins.*

CONCLUSIONS

In this work, we demonstrate a rapidly iterative approach to the development of a modular base for the fabrication of a 3D MEA. We utilized DLP 3D printing, due to its ability to resolve sensitive positive and negative 3D features, and characteristic low surface roughness. The novel micropillar through-via approach described herein enabled a conductive-epoxy casting method to produce higher aspect ratio through-vias, which also served as supports for batch-transitioned 3D electrodes. The final 3D MEA platform was characterized for its design to device translation, utilizing several imaging-based characterization methods. All crucial and sensitive negative relief features were well within reasonable error margins. Additionally, the final fabricated 3D MEA device was characterized for its *in situ* electrical performance, through full spectrum impedance and phase sweeps, both before and after electroplating of nano-porous platinum.

ACKNOWLEDGEMENTS

The authors would like to acknowledge the funding provided through NSF I/UCRC, NIH UG3TR003150 and NIH R43ES029886 grants, as well as through the UCF ORC Doctoral Fellowship (C. M. Didier), and the startup funding of Prof. Rajaraman.

REFERENCES

[1] W. Anderson et al., *"Advances in 3D neuronal microphysiological systems: towards a functional nervous system on a chip,"* In Vitro Cellular & Developmental Biology-Animal, 2021.

[2] J. Choi, et al., *"Recent advances in three-dimensional microelectrode array technologies for in vitro and in vivo cardiac and neuronal interfaces,"* Biosensors and Bioelectronics, 2021.

[3] C. Didier, et al. *"Development of in vitro 2D and 3D microelectrode arrays and their role in advancing biomedical research,"* Journal of Micromechanics and Microengineering, 2020.

[4] U. Robles et al., *"3-D printed structures by microdispensing materials loaded with dielectric and magnetic powders,"* IEEE Transactions on Components, Packaging and Manufacturing Technology, 2018.

[5] G.Shao et al., *"High-resolution 3D printing magnetically-active microstructures using micro-CLIP process,"* Nano-, Bio-, Info-Tech Sensors and 3D Systems III, 2019.

[6] S. F. Shiba et al., *"3D microlithography using an integrated system of 5-mm uv-leds with a tilt-rotational sample holder,"* Micromachines, 2020.

[7] M. Tirado et al., *"Digital light processing (DLP) 3D printing of millimeter-scale high-aspect ratio (HAR) structures exceeding 100: 1,"* 33rd IEEE International Conference on Micro Electro Mechanical Systems (MEMS), 2020.

[8] C. Didier et al., *"Rapid Makerspace Microfabrication and Characterization of 3D Microelectrode Arrays (3D MEAs) for Organ-on-a-Chip Models,"* Journal of Microelectromechanical Systems, 2021.

[9] C. Hart et al., *"Biocompatibility of blank, post-processed and coated 3D printed resin structures with electrogenic cells,"* Biosensors, 2020.

[10] J. Fuh et al., *"Post-cure shrinkage of photo-sensitive material used in laser lithography process,"* Journal of materials processing technology, 1997.

[11] S. Rajaraman et al., *"Fabrication of 3d microelectrodes and use thereof in multi-functional biosystems,"* U.S. Patent Application No. 16/908,666., 2021.

[12] B.S. Covino et al., *"Dissolution behavior of 304 stainless steel in HNO3/HF mixtures,"* Metallurgical Transactions A, 1986.

[13] N. Azim et al., *"Fabrication and characterization of a 3D printed, microelectrodes platform with functionalized electrospun nano-scaffolds and spin coated 3D insulation towards multi-functional biosystems,"* Journal of Microelectromechanical Systems. 2019.

[14] W. Franks et al., *"Impedance characterization and modeling of electrodes for biomedical applications,"* IEEE Transactions on Biomedical Engineering, 2005.

[15] D. Borkholder. *"Cell-based biosensors using microelectrodes,"* Stanford University Thesis, 1999.

CONTACT

*Swaminathan Rajaraman, tel: +1-407-823-4339; Swaminathan.Rajaraman@ucf.edu